SLIGHT AND MODERATE SALINE AND SODIC SOILS CHARACTERIZATION IN IRRIGATED AGRICULTURAL LAND USING MULTISPECTRAL REMOTE SENSING

A. BANNARI [1], A.M. GUEDON [1], A. EL-HARTI [2], F.Z. CHERKAOUI [3], A. EL-GHMARI [2] AND A. SAQUAQUE [4]

[1] Remote Sensing and Geomatics of Environment Laboratory, Department of Geography, University of Ottawa, Ottawa (Ontario) K1N 6N5 Canada, Phone (613) 562-5800 (Ext. 1042), Fax (613) 562-5145, Email: abannari@uottawa.ca
[2] Laboratoire de Télédétection et des SIG, Faculté des Sciences et Techniques, Béni-Mella, Morocco
[3] Laboratoire de Télédétection et SIG, Office Régional de Mise en Valeur Agricole du Tadla (ORMVAT), Fkih-Ben-Salah, Morocco
[4] Reminex, Managem Groupe Minier de l'ONA, Marrakech, Morocco

Commission VI, WG VI/4

KEY WORDS: Salinity, Sodicity, Electrical conductivity, Remote sensing, Spectral indices, spectroradiometric data, EO-1 ALI sensor.

ABSTRACT:

Around the world, especially in semi-arid regions, millions of hectares of irrigated agricultural land are abandoned each year because of the adverse effects of irrigation, mainly secondary salinity and sodicity. Accurate information about the extent, magnitude, and spatial distribution of salinity and sodicity will help create sustainable development of agricultural resources. In Morocco, south of the Mediterranean region, the growth of the vegetation and potential yield are limited by the joint influence of high temperatures and water deficit. Consequently, the over use of surface and ground water, coupled with agricultural intensification, generates secondary soils salinity and sodicity. This research focuses on the potential and limits of the Advance Land Imaging (EO-1 ALI) sensor spectral bands for the discrimination of slight and moderate soils salinity and sodicity in the Tadla's irrigated agricultural perimeter, Morocco. In order to detect affected soils, empirical relationships (second order regression analysis) were calculated between the electrical conductivity (EC) and different spectral salinity indices. To achieve our goal, spectroradiometric measurements (350 to 2500 nm), field observation, and laboratory analysis (EC of a solution extracted from a water-saturated soil, and soil reaction (pH)) were used. The spectroradiometric data were acquired using the ASD (*Analytical Spectral Device*) above 28 bare soil samples with various degrees of soils salinity and sodicity, as well as non-affected soils. All of the spectroradiometric data were resampled and convolved in the solar-reflective spectral bands of EO-1 ALI sensor. The results show that the SWIR region is a good indicator of, and are more sensitive to, different degrees of slight and moderate soil salinity and sodicity. In general, relatively high salinity soils show higher spectral signatures than do sodic soils and non-affected soils. Also, strongly sodic soils present higher spectral responses than moderately sodic soils. However, in spite of the improvement of EO-1 ALI spectral bands by comparison to Landsat-ETM+, this research shows the weakness of multi-spectral systems for the discrimination of slight and moderate soils salinity and sodicity. Although remote sensing offers a good potential for mapping strongly saline soils (dry surface crust), slight and moderately saline and sodic soils are not easily identified, because the optical properties of the soil surfaces (color, brightness, roughness, etc.) could mask the salinity and sodicity effects. Consequently, their spatial distribution will probably be underestimated. According to the laboratory results, the proposed Soils Salinity and Sodicity Indices (SSSI) using EO-1 ALI 9 and 10 spectral bands offers the most significant correlation (52.91 %) with the ground reference (EC). They could help to predict different spatial distribution classes of slight and moderate saline and sodic soils using EO-1 ALI imagery data.

1. INTRODUCTION

The increased use of ground and surface water coupled with the agricultural intensification in the Tadla's irrigated perimeter, Morocco, are the major cause of soil degradation through secondary soil salinity and sodicity. It is common that both saline and sodic conditions occur together.

Sodicity represents the amount of exchangeable sodium (Na+) in water and in soil. Sodicity in soils has a strong influence on the soil structure. Dispersion occurs when the clay particles swell strongly and separate from each other on wetting. On drying, the soil becomes dense, cloddy and without structure (Charters, 1993; Ford *et al.,* 1993; Sumner *et al.,* 1998). Sodic soils have a pH > 8.2 and a preponderance of carbonate and sodium by bicarbonate (Richards, 1954).

Salinity refers to the amount of soluble salt in soil, such as sulphates (SO_4), carbonates (CO_3) and chlorides (Cl). Strongly saline soils often exhibit a whitish surface crust when dry. The solubility of calcium sulphate, also called gypsum ($CaSO_4$), is used as the standard for comparing salinity levels. Unlike sodicity, water movements influence salinity. It occurs in areas where saline ground waters are very close to or at the ground surface, and evaporation exceeds precipitation (Dehaan and Taylor, 2002). In irrigated lands, salinity occurs when salts are concentrated in soils by the evaporation of freestanding irrigation water. The major causes are a combination of poor land management and crude irrigation practices. These practices cause changes in soil and vegetation cover and ultimately loss of vegetation and agricultural productivity. Soil salinity is measured by ground-based geophysics, measurements of soil electrical conductivity (EC) using soil pastes, and water ex-

tracts. Saline soils have an EC > 4 dS m^{-1} at 25°C and a pH < 8.2 (Richards, 1954).

Knowing when, where and how salinity and sodicity may occur is very important to the sustainable development of any irrigated production system (Al-Khaier, 2003). Remedial actions require reliable information to help set priorities and to choose the type of action that is most appropriate in each situation (Metternicht and Zinck, 2003). Ground-based electromagnetic measurements of soil EC are generally accepted as the most effective method for quantification of soil salinity (Norman *et al.,* 1989; cited in Dehaan and Taylor, 2002). Unfortunately, these methods are expensive, time consuming, and need considerable human resources for land surveying. Moreover, the dynamic nature of soil salinity and sodicity in space and time makes it more difficult to use conventional methods for comparisons over large areas (IDNP, 2002). A major challenge of remote sensing, as a potential alternative technique, is to detect different levels of soil salinity and sodicity (Fraser and Joseph, 1998; Taylor *et al.,* 1994). In fact, a large variety of remote sensing techniques have been used for identifying and monitoring salt-affected zones, including aerial photos, spectroradiometric measurements, multispectral, hyperspectral, passive and active microwave images (Chaturvedi *et al.,* 1983; Singh and Srivastav, 1990; Hick and Russel, 1990; Taylor *et al.,* 1996; Metternicht, 1998; Dehaan and Taylor, 2002; Metternicht and Zinck, 2003).

The objective of this research is to analyze, for the first time, the potential and limits of the Advance Land Imaging (EO-1 ALI) sensor spectral bands for the discrimination of slight and moderate secondary soil salinity and sodicity in the Tadla's irrigated agricultural perimeter, Morocco. Empirical relationships (second order regression analysis) were calculated between the EC and different spectral salinity indices to detect slight or moderate soil salinity and sodicity. In order to achieve our goal, spectroradiometric measurements (350 and 2500 nm), field observations, and laboratory analysis (EC of a solution extracted from a water-saturated soil, and soil reaction (pH)) were used. The spectroradiometric data were acquired during the summer season using the ASD (*Analytical Spectral Device*) above 28 bare soil samples with various levels of salinity and sodicity, as well as non-affected soils. All of the spectroradiometric data were resampled and convolved to match the solar-reflective spectral bands of the EO-1 ALI sensor using the updated Herman transfer radiative code, H5S (Teillet and Santer, 1991).

2. MATERIAL AND METHOD

2.1. Study site

The irrigated agricultural land of the Tadla region is one of the most important in Morocco. It is situated 30 km from the city of Béni-Mellal, at foot of the middle Atlas Mountains, and about 200 km south-east of Casablanca (32º 21' N, 6º 21' W; Figure 1). The primary crops are grains, legumes and sugar beets. Covering an area of 3600 km^2 and being at an average altitude of 400 m, the Tadla plain is bordered to the north by the phosphate plateau, to the south by the middle Atlas Mountains of Béni-Mellal, and to the east it narrows as it follows the Oum-El-Rbia river. The river divides the irrigated perimeter into two sub-perimeters with different hydrological and hydrogeologic characteristics: Béni-Amir and Béni-Moussa (Hammani *et al.,* 2004; Bellouti *et al.,* 2002). The sub-perimeter of Béni-Moussa has been irrigated since 1954 with good quality water from Bin-El-Ouidane dam (0.3 g l^{-1} of calcite, halite and gypsum).

Béni-Amir has been irrigated since 1938 by water from Oum-El-Rbia river, and show a salinity level of 2 g l^{-1} (mostly calcite and halite). Historically, the Tadla's irrigated perimeter has gone through two periods in the evolution of its water resources. The first period, from 1938 to 1980, was characterized by an abundance of surface water. The second period started in 1981 with a persistent drought that continues to the present day, and is defined by a large water shortage (Hammani *et al.,* 2004). Indeed, because of the impact of climate change (higher temperatures and water deficit), with its average annual rainfall under 350 mm and an average annual evapotranspiration of 1800 mm, the region has become semi-arid. It shows the characteristics of vulnerable Mediterranean landscapes with respect to the processes of soil impoverishment and environmental degradation. Consequently, recourse to underground water resources has become essential, even though the water qualities are poor. Increasing ground water use causes soil salinity and sodicity to become more pronounced in important areas of the Tadla plain (Debbarh and Badraoui, 2002).

2.2. Soils sampling and laboratory analysis

Four different soil classes characterize the Tadla irrigated perimeter. The "iso-humiques" class, which contains medium brown subtropical soils, saline and saline-sodic brown subtropical soils, and medium chestnut soils. This class is the most dominant in the perimeter, representing about 83 % of soils. The class of "calcimagnesique" soils includes brown limestone's (11%), and "rendziniforme" soils. The class of "ferralitiques" soils with iron sesquioxides and the hydro-morphs soils class are poorly evolved (Bellouti *et al.,* 2002).
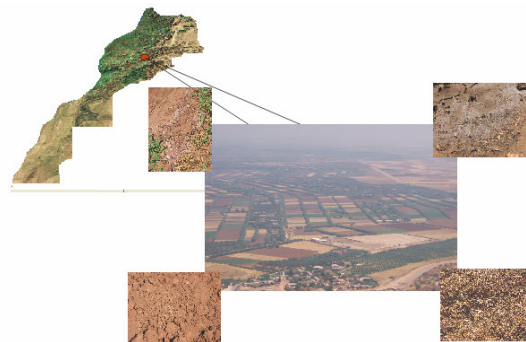
Figure 1: Study site, Tadla's irrigated agricultural perimeter (Béni-Mellal, Morocco)

Soils data collection was carried out during the dry season, between August 25 and September 5 2005, in the Tadla's irrigated agricultural perimeter. The soil sampling data consisted of 28 samples which were selected on the basis of the spatial representativeness of the major soil types, and various degrees of salinity and sodicity (Table 1). Samples were taken from the soils upper layer (5 cm depth). Observations and remarks about each sample (color, brightness, texture, etc.) were noted. The location of each point was recorded with a global positioning system (GPS) unit, and photographed using a 35 mm digital camera equipped with a 28 mm lens.

The laboratory analyses consisted of EC extracted from a soil with a water-saturated past, and soil reaction (pH). These elements were analyzed in the laboratory using the current interna-

tional standards methods in soil science (Baize, 1988). Based on the results of our analyses, and according to Metternich and Zinck (1997), we established three salinity classes using EC (non saline: 0 to 4 dS m^{-1}, slight: 4 to 8 dS m^{-1}, and moderate: 8 to 16 dS m^{-1}), and three sodicity classes using pH (slight: 7 to 8 pH, moderate: 8 to 8.5 pH, and strong: 8.5 to 9 pH). Seven informational classes resulted from the combination of salinity and sodicity classes (Table 1).

Salinity & Sodicity Class	Soil	EC	pH
Moderate salinity & Slight sodicity	4"	8.28	8.0
	7	11.06	7.8
	9	11.19	8.2
	11	10.42	8.0
	18	9.68	8.0
Moderate salinity & Moderate sodicity	17	14.58	8.1
Slight salinity & Moderate sodicity	10	5.83	8.1
	21	6.17	8.0
Slight salinity & Strong sodicity	16	5.87	8.5
	22	4.2	8.68
Non saline & Slight sodicity	3'	0.97	8.0
	5	0.85	8.0
	6	1.72	8.0
	8	3.33	7.8
	12	2.22	8.0
	14	1.76	8.0
	24	0.57	7.94
	25	1.88	7.7
	27	0.79	7.83
Non saline & Moderate sodicity	1	1.8	8.2
	2'	0.66	8.1
	13	2.94	8.4
	19	2.44	8.1
	23	0.69	8.21
	26	0.86	8.25
	28	1.45	8.01
Non saline & Strong sodicity	15	0.77	8.51
	20	1.52	8.5

Table 1: Informational classes resulted from the combination of salinity and sodicity classes

2.3. Spectroradiometric measurements

After the soil sampling and before the laboratory analysis, spectroradiometric measurements were acquired above the 28 bare soil samples using the ASD spectroradiometer (ASD Inc, 1999). This instrument is equipped with three detectors operating in the visible, NIR and SWIR, between 350 and 2500 nm. It allows a continuous spectral signature with 1.4 nm sampling step in the areas from 350 to 1000 nm and 2 nm in the areas of 1000 to 2500 nm. The system resamples the measurements with a 1 nm step, which allows the acquisition of 2151 contiguous bands per spectrum. The sensor is characterized by the programming capacity of the integration time, which allows an excellent performance of the signal-to-noise ratio, as well as a great stability. Measurements were taken at the laboratory using two halogen lamps of 500 W each, equipped with an electrical current regulator. The data were acquired at nadir with a FOV (Field of View) of 25° and an illumination angle approximately 5° from the vertical. The spectroradiometer was installed on a tripod at

a height of approximately 30 cm from the target, which made it possible to observe a surface area of 177 cm[2]. A laser beam was used to locate the center of the ASD FOV compared to the center of each sample. The reflectance factor of each soil sample was calculated in accordance with the method described by Jackson *et al.* (1980) by rationing target radiance to the radiance obtained from a calibrated 25-cm by 25-cm white Spectralon panel (Labsphere, 2001). Corrections were made for the wavelength dependence and non-Lambertien behavior of the panel. The Spectralon radiance was acquired immediately prior to the target radiance. The average of 25 spectra was convolved in the solar-reflective spectral bands of EO-1 ALI sensor using the updated Herman transfer radiative code, H5S (Teillet and Santer, 1991).

2.4 ALI sensor

Launched in November 2000, the Advance Land Imaging (ALI) is the first Earth-Observing (EO-1) sensor to be flown under NASA's New Millennium Program. This sensor was designed as a technology validation instrument for the next generation of Landsat-like instruments. It is a push-broom sensor that employs linear array technology, which is geometrically more stable than the cross-track scanning of MSS, TM and ETM+ systems (Ungar, 2001). This stability allows a simpler, less time-dependent geometric modeling approach but brings with it new challenges associated with the increased focal plane complexity (Storey *et al.,* 2004). Indeed, ALI employs novel wide-angle optics and highly integrated multispectral and panchromatic spectrometers. It uses a triplet telescope with visible, near infrared and shortwave infrared focal planes. The instrument focal plane is partially populated with four sensor chip assemblies (SCA) and each covers 3° by 1.625° (NASA, 2006). Each of the four SCAs contains 320 detectors (i.e. pixels) in the cross-track direction. For the panchromatic band, each SCA contains 960 detectors in the cross-track direction. There is an overlapping coverage of approximately 10 detectors between each adjacent pair of SCAs for the multispectral bands. For the panchromatic band, there is a coverage overlap of approximately 30 detectors between each adjacent pair of SCAs (NASA, 2006). Operating at an orbit of 705 km, the EO-1 ALI across-track ground swath width is 37 km and the along-track length is normally 42 km. The pixel size is very similar to Landsat-7 ETM+, except for the higher-resolution (10 meters) in the panchromatic (band 1) for ALI, and 30 meters in all other bands, 2 to 10 (NASA, 2006). Five bands mimic the ETM+ bands 1, 2, 3, 5, and 7. ETM+ band 4 is split into two bands covering 775 - 805 nm and 845 - 890 nm. In addition, there are two new additional bands labeled 2 and 8 at 433 - 453 nm and 1200 - 1300 nm, respectively, with 30 m pixel size (Bicknell *et al.,* 1999). Table 2 presents the spectral bands of the EO-1 ALI sensor and their respective wavelengths.

Band	Wavelength (nm)	Band	Wavelength (nm)
1*	480 – 690	6	775 – 805
2	433 – 453	7	845 – 890
3	450 – 515	8	1200 – 1300
4	525 – 605	9	1550 – 1750
5	630 – 690	10	2080 – 2350

* Panchromatic band

Table 2: Spectral bands of EO-1 ALI sensor

2.5. Salinity indices

In the literature, different spectral salinity indices are proposed for salt mineral detection and identification, at least when they are the dominant soil constituent. To retrieve information on the salt-affected areas from the LISS-II sensor of the IRS-1B satellite, Khan *et al.* (2001) proposed three spectral salinity indices: the Brightness index (BI), Normalized Difference Salinity Index (NDSI) and Salinity Index (SI). Among these indices, they found that NDSI provided satisfactory results retrieving different salt classes. According to Al-Khaier (2003), the ASTER salinity index (ASTER-SI), which uses bands 4 and 5, accurately detects overall salinity in bare agricultural soils. A methodology was proposed by the Indo-Dutch Network Project (IDNP, 2002) for identification of soil salinity conditions using remote sensing Landsat-TM system and GIS. Amongst several remote sensing techniques, this project proposes three different salinity indices: SI-1, SI-2 and SI-3. The last is similar to the ASTER-SI index. In this research, all these indices were considered, calculated in EO-1 ALI spectral bands, and tested for the detection of slight and moderate soil salinity and sodicity effects.

$$BI = \sqrt{ALI5^2 + ALI6^2} \qquad (1)$$

$$NDSI = (ALI5 + ALI7)/(ALI5 + ALI7) \quad (2)$$

$$SI = \sqrt{ALI3 * ALI5} \qquad (3)$$

$$ASTER\text{-}SI = (ALI9 - ALI10)/(ALI9 + ALI10) \qquad (4)$$

$$SI\text{-}1 = (ALI9)/(ALI10) \qquad (5)$$

$$SI\text{-}2 = (ALI6 - ALI9)/(ALI6 + ALI9) \qquad (6)$$

$$SI\text{-}3 = (ALI9 - ALI10)/(ALI9 + ALI10) \qquad (7)$$

3. RESULTS AND DISCUSSION

Soil spectral signatures can provide information on the soil properties and quality. Indeed, there is a high correlation between soil reflectance and soil properties such as organic matter content, moisture content, mineral composition, iron oxide content, color, brightness, roughness, size and shape of the soil aggregate, and the salt and sodium content. Figure 2 illustrates the spectral signature of the soils measured for this study. In general, this figure illustrates that moderately saline soils show higher spectral signature than do sodic and non-affected soils. Strongly sodic soils show higher spectral response than do moderately sodic soils. Non-affected soils, which have good structure and high organic matter, show very low spectra. Indeed, moderately saline soils are relatively smoother than soils with good structure, and cause high reflectance in the visible and near infrared bands, especially when soil is dry. These observations are very clear when we resample the data in the EO-1 ALI sensor spectral bands and we compare various degrees of soil salinity and sodicity and vegetation cover (Figure 3). This figure also shows that the spectral properties of the soils salinity and sodicity are detectable in the visible and near infrared, but are most evident in the SWIR region. However, in spite of this capability, the color, brightness and the roughness of the soil surfaces have a strong impact on the spectral signature (Figure 4). For instance, after irrigation the fine soil surfaces become dry, smooth and change the optical properties. As well, the spatial distribution of particles size, the roughness and the texture of the soil surfaces change. Consequently, the spectral signature of soil increases automatically, and masks moderate or slight salinity and sodicity effects (Figures 2 and 4). Even if

the spectral reflectance in the near infrared and SWIR wavelengths provides a rapid and expressive means of characterizing strongly saline and sodic soils, it is probable that spectral confusion occurs between moderate or slightly saline and sodic soils, and non-affected soils with bright and clear color. For instance, soils 3' and 6 show the same level of salinity and sodicity, but their spectral signature are different because of the difference of their optical proprieties (Figure 4 and Table 1). Although soil 6 is non-saline with slight sodicity (good structure with organic matter) its signature is similar to that of soil 11, which is moderately saline. The spectral signature of soils 7 and 16 are alike but not their degrees of salinity and sodicity, or their color. These observations are in agreement with other research using field or laboratory analysis, or testing other satellite sensors (Chapman *et al.,* 1989; Hick and Russel, 1990; Crowley, 1991; De Jong, 1992; Mougenot *et al.,* 1993; Rao *et al.,* 1995; Metternicht and Zinck, 1997; Goldshleger *et al.,* 2001). Furthermore, even if the saline soil can be characterized by having different absorption features, Figure 2 shows that it is not possible to characterize, or to distinguish between, slight or moderate saline and sodic soils by their absorption features. This was not expected because the salt and sodium content status was not very strong in the soil samples and, consequently, these absorption features are absent.
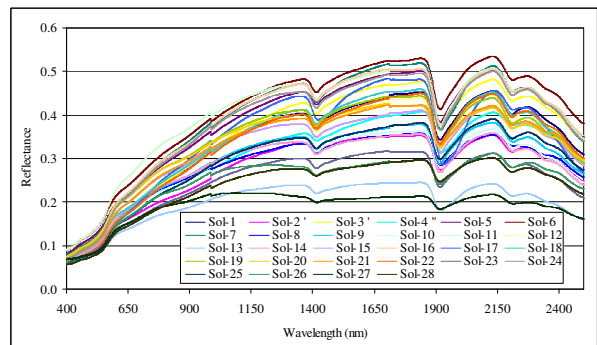

Figure 2: Spectral signatures of the considered soils.
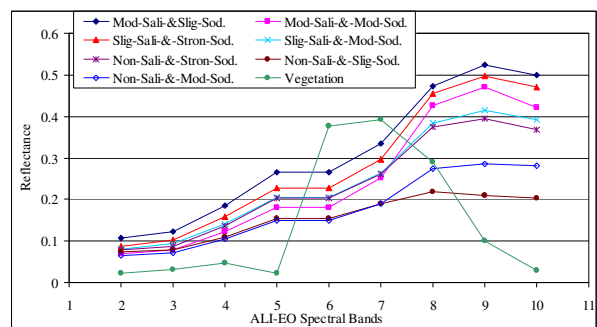
Figure 3: Resampled and convolved spectra in EO-1 ALI spectral bands for vegetation, non-affected soil, slight and moderate saline soils, and sodic soil.

To detect slight and/or moderate saline and sodic affected soils, empirical relationships (second order regression analysis) were undertaken between the EC (ground reference) and different spectral salinity indices. Table 2 presents the resulting correlation coefficients. Among the indices proposed in the literature, only the ASTER-SI (similar to SI-3) provides the highest corre-

lation (46.9 %) especially when we consider just the saline and sodic soils. However, this correlation is not significant enough to retrieve accurate information. Khan *et al.* (2001) found that NDSI provides satisfactory results retrieving different salt classes (dry surface crust), but the research here shows that this index offers a very low correlation coefficient of 22.82% (especially when we consider all soils). If we take into account only the affected soils, this coefficient increases to 42.69 %. The other indices show their limitation and a very low potential discrimination between slight and moderate soil salinity and sodicity effects, and non-affected soils.
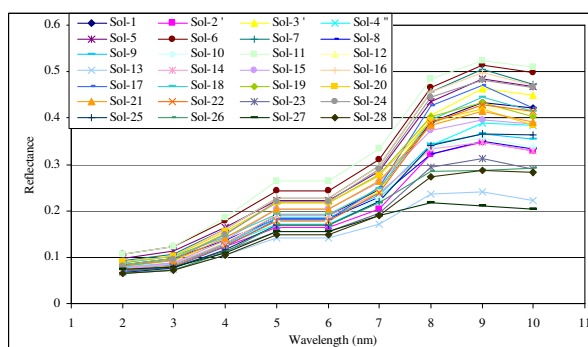

Figure 4: Resampled and convolved spectra in EO-1 ALI spectral bands

Salinity Index	Correlation coefficient (%)	
	All soils	Only saline and sodic soils
SI	4.53	5.65
BI	6.63	2.21
SI-1	18.86	46.70
SI-2	12.88	36.07
SI-3	18.59	46.90
ASTER-SI	18.6	46.90
NDSI	22.82	42.69
SSSI-1	34.00	52.00
SSSI-2	34.21	52.91

Table 2: Correlation coefficient between EC and spectral soil salinity indices

Furthermore, when we correlate EC with the reflectances in each of the EO-1 ALI spectral bands, bands 9 and 10 provide the highest correlation. Using these two SWIR spectral bands, we devised soil salinity and sodicity indices (SSSI). SSSI-1 uses a simple difference between spectral bands 9 and 10, whereas SSSI-2 uses a normalized difference ratio. These empirical relationships are more useful than individual spectral bands or the other indices. They offer a correlation coefficient of 52.91% with the EC using a second order regression analysis. This correlation is not so high, but it's the most significant one compared to the other indices (Table 2). According to these laboratory results, we note that in spite of this correlation, which is at the acceptable limit, the SSSI-1 and SSSI-2 could enhance the slight and moderate saline and sodic zones, and differentiate them from non-affected soils using EO-1 ALI imagery data.

$$SSSI\text{-}1 = (ALI9 \quad - \quad ALI10) \qquad (8)$$
$$SSSI\text{-}2 = (ALI9 * ALI10 \quad - \quad ALI10 * ALI10)/ALI9 \quad (9)$$

4. CONCLUSIONS

This research focused on the potential and limits of the Advance Land Imaging (EO-1 ALI) sensor spectral bands for the discrimination of slight and moderate soil salinity and sodicity in the Tadla's irrigated agricultural perimeter, Morocco. The results show that the SWIR region is a good indicator, being more sensitive to different degrees of slight and moderate soil salinity and sodicity. In general, relatively high salinity soils show higher spectral signatures than do sodic soils and non-affected soils. Also, strongly sodic soils present higher spectral responses than moderately sodic soils. However, in spite of the improvement of EO-1 ALI sensor spectral bands characteristics in comparison to Landsat-ETM+, this research shows the limitation of multi-spectral systems for slight and moderate soil salinity and sodicity discrimination. Although remote sensing offers a good potential for mapping strongly saline soils (dry surface crust), slight and moderate saline and sodic soils are not easily identified, because the optical proprieties of the soils surfaces (color, brightness, roughness, etc.) could mask the salinity and sodicity effects. Consequently, their spatial distribution will probably be under-estimated. To detect slight and moderate soil salinity and sodicity effects, the Soils Salinity and Sodicity Indices (SSSI) using ALI spectral bands 9 and 10, offer the most significant correlation (52.91%) with the ground reference (EC). Even if this correlation is not so high, they could help to predict different spatial distribution classes of slight and moderate saline and sodic soils using EO-1 ALI imagery data.

REFERENCES
Al-Khaier, F., 2003. Soil Salinity Detection Using Satellite Remotes Sensing. Master's thesis, International institute for Geo-information science and earth observation, Enschede, The Netherlands. 61 pages.

Analytical Spectral Devices, ASD Inc., 1999. http://www.asdi.com/products-spectroradiometers.asp

Baize, D., 1988. Guide des analyses courantes en pédologie: choix expression, presentation et interpretation. INRA, Paris, France.

Bellouti, A., Cherkaoui, F., Benhida, M., Debbarh, A., Soudi, B. et Badraoui, M., 2002. Mise en place d'un système de suivi et de surveillance de la qualité des eaux souterraines et des sols dans le périmètre irrigué du Tadla au Maroc. In Marlet, S. et Ruelle, P. (éditeurs): Vers une maîtrise des impacts environnementaux de l'irrigation. *Actes de l'atelier du PCSI*, Montpelier, France. 11 pages.

Bicknell, W.E., Digenis, C.J., Forman, S.E. and Lencioni, D.E., 1999. EO-1 advanced land imager. *Proceedings of SPIE*, Vol. 3750, pp. 80 - 88.

Chapman, J.E., Rothery, D.A., Francis, P.W. and Pontual, A., 1989. Remote sensing of vaporite mineral zonation in salt flats (salars). *International Journal of Remote Sensing*, 10, pp. 245 - 255.

Chartres, C.J., 1993. Sodic soils: an introduction to their formation and distribution in Australia. *Australian Journal of Soil Research,* 31, pp. 751 - 760.

Chaturvedi, L., Carver, K., Clifford Harlan, J., Hancock, G., Small, F. and Dalstead, K., 1983. Multispectral remote sensing of saline seeps. *IEEE Transactions on Geoscience and Remote Sensing*, 21, pp. 231 - 239.

Crowley, J.K., 1991. Visible and near-infrared (0.4-2.5 μm) reflectance spectra of playa evaporite minerals. *Journal of Geophysical Research*, 96(16), pp. 231- 240.

Debbarh, A. and Badraoui, M. 2002. Irrigation et environnement au Maroc : situation actuelle et perspectives. In Marlet, S. et Ruelle, P. (éditeurs): Vers une maîtrise des impacts environnementaux de l'irrigation. *Actes de l'atelier du PCSI*, Montpelier, France. 14 pages. http://doc.abhatoo.net.ma/doc/IMG/pdf/irrig.pdf

De Jong, S. (1992) The analysis of spectroscopical data to map soil types and soil crusts of Mediterranean eroded soils. *Soil Technology*, 5, pp. 199 - 211.

Dehaan, R.L. and Taylor, G.R., 2002. Field-derived spectra of salinized soils and vegetation as indicators of irrigation-induced soil salinization. *International Journal of Remote Sensing*, 80, pp. 406 - 417.

Drake, N. A., 1995. Reflectance spectra of evaporate minerals (400-2500 nm): applications for remote sensing. *International Journal of Remote Sensing*, 16, pp. 2555 - 2571.

Ford, G.W., Martin, J.J., Rengasamy, P., Boucher, S.C. and Ellington, A., 1993. Soil sodicity in Victoria. *Australian Journal of Soil Research,* 31, pp. 869 - 909.

Fraser, D. and Joseph, S., 1998. Mapping soil salinity in the Murray Valley (NSW) using satellite imagery. *Proceedings of the 9th Australasian Remote Sensing and Photogrammetry Conference*, Sydney, Australia. Paper published on CD.

Goldshleger, N., Ben-Dor, E., Benyamini, Y., Agassi, M. and Blumber, D., 2001. Characterization of soil's structural crust by spectral reflectance in the SWIR region (1.2 – 2.5 μm). *Terra Nova*, 13, pp. 12 - 17.

Hammani, A., Kuper, M., Debbarh, A., Bouarfa, S., Badraoui, M. et Bellouti, A., 2004. Evolution de l'exploitation des eaux souterraines dans le périmètre irrigué du Tadla. *Actes du séminaire sur la modernisation de l'agriculture irriguée*, Rabat, Maroc. 8 pages.

Hick, P.T. and Russel, W.G.R., 1990. Some spectral considerations for remote sensing of soil salinity. *Australian Journal of Soil Research*, 28, pp. 417-431.

IDNP, 2003. Indo-Dutch Network Project: A Methodology for Identification of Waterlogging and Soil Salinity Conditions Using Remote Sensing. Central Soil Salinity Research Institute, Karnal, India, 78 pages.

Jackson, R.D. Pinter, P.J., Paul, J., Reginato, R.J., Robert, J. and Idso, S.B., 1980. Hand-held Radiometry. U.S. Department of Agriculture Science and Education Administration, Agricultural Reviews and Manuals, ARM-W-19, Phoenix, Arizona, U.S.A.

Khan, N.M., Rastoskuev, V.V., Shalina,E.V. and Sato,Y., 2001. Mapping Salt-Affected Soils using remote sensing Indicators – A simple approach with the use of GIS IDRISI. *Proceedings of the 22nd Asian Conference on Remote Sensing*, 5-9 November, Singapore. Center for Remote Imaging, sensing and Processing (CRISP), National University of Singapore; Singapore Institute of Surveyors and Valuers; Asian association on remote sensing.

Labsphere, 2001. A guide to reflectance coatings and materials. North Sutton, NH., http://www.labsphere.com/tech_info/docs/Coating_&_Material_Guide.pdf.

Metternicht, G. I., 1998. Fuzzy classification of JERS-1 SAR data: an evaluation of its performance for soil salinity mapping. *Ecological Modelling*, 111, pp. 61 - 74.

Metternicht, G.I. and Zinck, J.A., 2003. Remote sensing of soil salinity: potentials and constraints. *Remote sensing of the environment*, 85, pp. 1 - 20.

Metternicht, G. I. and Zinck, J. A., 1997. Spatial discrimination of salt- and sodium-affected soil surfaces. *International Journal of Remote Sensing*, 18, pp. 2571 - 2586.

Mougenot, B., 1993. Effets des sels sur la réflectance et télédétection des sols salés. Cahiers ORSTOM, Série Pédologie, 28, pp. 45 - 54.

NASA, 2006. Earth Observing 1 (EO-1) User's Guide. http://eo1.usgs.gov/userGuide/index. html.

Norman, C.P., Lyle, C.W., Heuperman, A.F. and Poulton, D., 1989. Tragowel Plains – Challenge of the Plains. In: Tragowel Plains Salinity Management Plan, Soil Salinity Survey, Tragowel Plains Subregional working group, pp. 49-89. Melbourne: Victorian, Department of Agriculture.

Rao, B., Sankar, T., Dwivedi, R., Thammappa, S., Venkataratnam, L., Sharma, R. and Das, S., 1995. Spectral behaviour of salt-affected soils. *International Journal of Remote Sensing,* 16, pp. 2125 - 2136

Richards, L.A., 1954. Diagnosis and improvements of saline and alkali soils. U.S. Salinity Laboratory DA, US Department of Agriculture Hbk 60, 160 pages.

Singh, R. P. and Srivastav, S. K., 1990. Mapping of waterlogged and saltaffected soils using microwave radiometers. *International Journal of Remote Sensing*, 11, pp. 1879 - 1887.

Storey, J.C., Choate, M.J. and Meyer, D.J., 2004. A Geometric Performance Assessment of the EO-1 Advanced Land Imager. *IEEE Transaction on Geosciences and Remote Sensing*, 42(3), pp. 602 - 607.

Sumner, M.E., Miller, W.P., Kookana, R.S. and Hazelton, P., 1998. Sodicity, dispersion, and environmental quality. In Sumner, M.E. and Naidu, R. (eds) "Sodic Soils - Distribution, Properties, Management and Environmental Consequences". Oxford University Press, New York, pp. 149 - 172.

Szabolcs, I., 1987. The global problems of salt-affected soils. *Acta Agronomica Hungarica*, 36, pp. 159 - 172.

Taylor,G. R., Mah, A. H., Kruse, F. A., Kierein-Young, K. S., Hewson, R. D. and Bennett, B. A., 1996. Characterization of saline soils using airborne radar imagery. *Remote Sensing of Environment*, 57, pp. 127 - 142.

Taylor, G.R., Bennett, B.A., Mah, A.H. and Hewson, R.D., 1994. Spectral properties of salinised land and implications for interpretation of 24 channel imaging spectrometry. *Proceedings of the first international remote sensing conference and exhibition*, Strasbourg, France, Vol. 3, pp. 504 - 513.

Teillet, P.M. and Santer, R.P. (1991) Terrain Elevation and Sensor Altitude Dependence in a Semi-Analytical Atmospheric Code. *Canadian Journal of Remote Sensing*, Vol. 17, No. 1, pp. 36-44.

Ungar, S.G., 2001. Overview of EO-1: the first 120 days. *Proceedings of IGARSS*, Vol. 1, pp. 43 - 45.